ELSEVIER

Thin Solid Films 299 (1997) 94–103

thin solid films

High quality optoelectronic grade epitaxial AlN films on α-Al_2O_3, Si and 6H-SiC by pulsed laser deposition [1]

R.D. Vispute [a], J. Narayan [a,*], J.D. Budai [b]

[a] *Department of Materials Science and Engineering, North Carolina State University, Raleigh, NC 27695-7916, USA*

[b] *Solid State Division, Oak Ridge National Laboratory, Oak Ridge, TN 37831-6030, USA*

Received 7 June 1996; accepted 30 September 1996

Abstract

AlN is one of the most important optoelectronic materials in the wide band gap III–V semiconductors because of its wide and tunable energy band gap in conjunction with other nitrides, high thermal conductivity, doping capabilities, and high hardness. The proposed optoelectronic devices require high quality epitaxial films on various substrates. Here, we present our recent work on the fabrication of high quality epitaxial AlN films on $Al_2O_3(0001)$, Si(111) and 6H-SiC(0001) by pulsed laser deposition (PLD). The PLD is a nonequilibrium technique where thin film growth temperature can be reduced by more than 250–350°C and epitaxial films comparable in quality to MOCVD (equilibrium technique) obtained. The laser fluence and the substrate temperature were found to be crucial processing parameters for the formation of high quality monocrystalline AlN films. The AlN films deposited above 750°C and laser energy densities of 2–3 J cm^{-2} were found to be epitaxial with *c*-axis normal to substrate plane. The X-ray rocking curve of epitaxial films on sapphire and SiC yielded full-width-at-half-maximum of ~0.06–0.07°. The transmission electron microscopy also revealed that the films were epitaxial with an orientational relationship of AlN[0001]‖Al_2O_3[0001], AlN[0001]‖Si[111], AlN[0001]‖SiC[0001] and in-plane alignment of AlN[$\bar{1}2\bar{1}0$]‖ Al_2O_3[$0\bar{1}10$], AlN[$10\bar{1}0$]‖Al_2O_3[$\bar{2}110$], AlN[$2\bar{1}\bar{1}0$]‖Si[$01\bar{1}$] and AlN[$0\bar{1}10$]‖SiC[$0\bar{1}10$]. The optical absorption edge measured by UV-visible spectroscopy for the epitaxial AlN film on sapphire was sharp and the band gap was found to be 6.1 eV. The electrical resistivity of the films was about $5–6 \times 10^{13}$ Ω cm^{-1} with a breakdown field of 5×10^6 V cm^{-1}. © 1997 Elsevier Science S.A.

Keywords: Aluminuim nitride; Epitaxy; Growth mechanism; Laser ablation

1. Introduction

Recent developments in heteroepitaxial growth of various electronic and optoelectronic materials on semiconducting and insulating substrates have enhanced the possibility of attaining a wide range of signal processing operations in monolithic structures. The ability to integrate compatible materials with different functional properties on a common substrate also offers the prospect of developing low cost, miniaturized, and high speed circuits and systems. The wide band gap III–V nitrides have assumed a leading role in view of their desired optoelectronic and thermal properties for high temperature and high power optoelectronic devices [1–3]. AlN, GaN and their alloys ($Al_xGa_{1-x}N$), are the most important materials in this context because of their wide and tunable energy band gaps, high thermal conductivity and doping capabilities [1–3]. Aluminum nitride (having hexagonal wurtzite structure, lattice constants are $a = 0.3112$ nm and $c = 0.4982$ nm), with a band gap of 6.2 eV and high surface acoustic wave (SAW) velocity (6×10^5 cm s^{-1}) offers tremendous potential for UV light emitting and SAW devices [2,4]. Additionally, AlN has a high thermal conductivity (320 W mK^{-1}) [5], high thermal stability (up to 2200°C) [6], high resistivity (10^{13} ohm cm^{-1}) [7], high dielectric strength (14 KV mm^{-1}) [8] and high chemical inertness [1,3]. AlN has also comparable lattice constants to that of GaN and hence epitaxial AlN layers are widely used as a template layer for 2D growth of GaN layers and also to reduce the lattice mismatch induced strains in the GaN films on sapphire substrates [9]. High quality epitaxial heterostructures are required to fully realize these microelectronics applications of AlN. The heteroepitaxial composite structures such as AlN on semiconductor and oxide insulator substrates are also of scientific interest because the epitaxy is determined by domain matching [10,11] rather than by lattice matching and interfacial chemical bonding characteristics of Al–N bonds. The degree of crystalline perfection of the deposits

* Corresponding author.

[1] Presented at the International Conference on Metallurgical Coatings and Thin Films, San Diego, CA, 22–26 April, 1996.

0040-6090/97/$17.00 © 1997 Elsevier Science S.A. All rights reserved
PII S0040-6090(96)09395-9

further depends largely on the chemical nature of the substrate surface in addition to the processing parameters such as substrate temperature, ambient gas pressure, etc. and method of deposition. Various techniques have been reported for the synthesis of AlN films [1–3]. These include chemical vapor deposition (CVD) [12], plasma assisted CVD [13], metal organic CVD [14], reactive d.c.-magnetron sputtering [15], plasma assisted molecular beam epitaxy (MBE) [16], laser CVD [17] and pulsed laser deposition (PLD) [10,11,18–21]. High quality epitaxial AlN films have been grown by conventional metalorganic CVD (MOCVD) and reactive MBE techniques employing high temperature growth processing in the range of 1050–1300°C [1–3,9,14,22]. There are only a few reports on the synthesis of AlN films on sapphire at relatively low temperatures between 300–800°C. These include switched atomic layer epitaxy (SALE) by Khan et al. [23], electron cyclotron resonance plasma assisted CVD by Zhang et al. [24] and reactive sputtering by Okano et al. [25].

PLD is emerging as a novel thin film growth technique for the synthesis of high quality epitaxial films at relatively low growth temperatures [26–29]. Particularly, in the context of fabrication of multicomponent ceramic thin films, PLD has been shown to be an excellent growth technique offering not only superior electrical and optical properties but also allows fabrication of integrated multilayer heterostructures by in-situ single chamber processing [29]. The highly nonequilibrium nature and stoichiometric ablation of the target material associated with the evolution (formation) of the plasma plume provide desirable characteristics for the fabrication of oxides, nitrides and a variety of multicomponent materials in thin film form. It is generally believed that the highly nonequilibrium nature of the process combined with the specific properties of the laser generated plasma plume (especially the high ions to atoms concentration ratio, and the energy of the generated species in the range of 10–100 eV) are responsible for the improved quality of the PLD films [27–29]. Over the past seven to eight years, PLD has been extensively employed for the preparation of thin films of oxides (high-T_c superconductors and related compounds, ferroelectric materials, $Y–ZrO_2$, MgO, CeO_2), nitrides (c-BN, TiN, CN_x), and carbides (TiC, SiC) [26–29]. Recently, we demonstrated that PLD technique can be used for the preparation of high quality epitaxial AlN films on sapphire (0001) [10] and Si(111) [11]. In this paper, we report our detailed work on processing and characterization of high quality optoelectronic grade epitaxial AlN films on Al_2O_3(0001), SiC(0001) and Si(111). The important growth parameters such as substrate orientation, surface preparation, growth temperature, laser parameters (fluence and repetition rate), ambient gas pressure etc. are optimized for obtaining heteroepitaxial growth of AlN. We show that the PLD is a low-temperature thin film processing because the average energy of particles in the laser evaporated species is considerably higher (~ 10 eV) than that of the thermal evaporation process (~ 0.1 eV) [27–29]. The additional energy during laser ablation is utilized in recrystallization of thin films.

2. Experimental

The AlN films were deposited inside a stainless steel vacuum system evacuated by a turbomolecular pump to a base pressure of 1×10^{-7} Torr. A schematic diagram of the PLD chamber is shown in Fig. 1. Radiation from a KrF excimer laser ($\lambda = 248$ nm, 25 ns pulse duration) was used to ablate the stoichiometric AlN target with laser energy densities (E_D) ranging from 2 to 15 J cm^{-2}. A stoichiometric hot pressed TiN target was also mounted on a rotating polygon for in-situ multilayer depositions and it was ablated at an E_D of ~ 10 J cm^{-2}. The target was irradiated by the laser through a quartz window at an angle of 45° with the target surface. The laser beam was focused on the target by using spherical lens having a focal length of 50 cm. The laser induced evaporated material was then allowed to condense on to the heated substrate kept at a distance of 5 cm from the target surface. Commercially available sapphire (0001), 6H-SiC(0001) and Si(111) substrates were first degreased with acetone and methanol. The sapphire substrates were thermally annealed at 1100°C in O_2 atm for 12 h. The Si(111) and 6H-SiC substrates were dipped into 10% HF solution before deposition. The films were grown at different substrate temperatures (T_s) ranging from 100–850°C with pulse repetition rates between 10 to 30 Hz for 9–10 min and nitrogen partial pressures ranging from 10^{-7} to 10^{-4} Torr. The laser beam was scanned during deposition by means of a moving mirror to achieve uniform film thickness over a 2.5×2.5 cm^2 area. The small spot size gave a plume that was less forward directed compared with larger spots and led to uniform films. The typical average growth rates of AlN films achieved in our experiments with the use of an E_D of 2–3 J cm^{-2} were in the range of 0.02 to 0.03 nm per pulse. The film thickness was ~ 200–250 nm.

The AlN films were characterized by Fourier transform infrared spectroscopy (FTIR), Raman spectroscopy, ultraviolet-visible (UV-V) spectroscopy, X-ray diffraction (XRD), transmission electron microscopy (TEM), and scanning electron microscopy (SEM). The electrical resistivity of the AlN films were measured for metal–insulator–metal structures at room temperature. Raman spectroscopy was carried out using green light (514.5 nm line) from an Ar^+ ion laser. The incident light was made grazing along the plane of the AlN film and the scattered light was collected in the direction normal to the substrate, i.e. along c-axis of the AlN film. We did not use any polarization analyzer for the scattered light. The scattered light was dispersed in a one meter 1704 Spex monochromator with a resolution of 0.4 cm^{-1} and the counts were taken for 1 min at each wavelength with a photomultiplier in photon counting mode. The detailed XRD studies (Θ, ω and Φ scans) were carried out by using a Rigaku rotating anode X-ray generator, a Huber four-circle

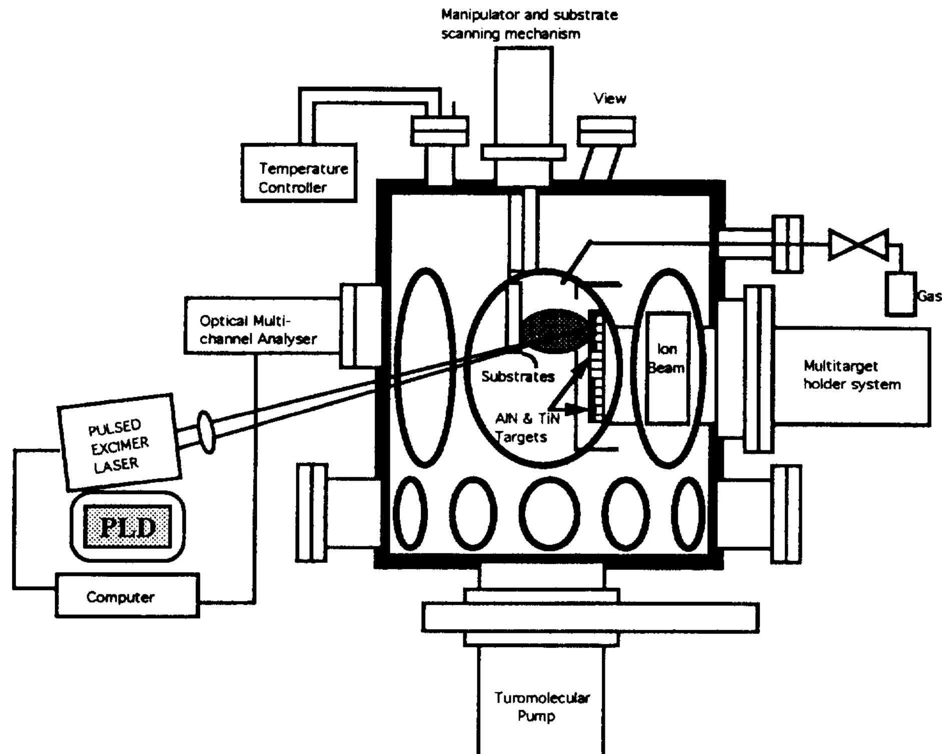

Fig. 1. Schematic diagram of the PLD system.

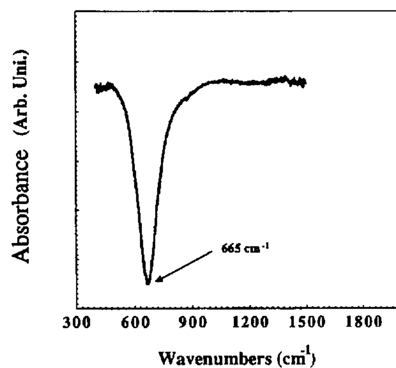

Fig. 2. FTIR spectrum of a ~200 nm AlN film deposited on Si(111) at E_D of 3 J cm^{-2}, T_s of 750°C and base pressure of 3×10^{-7} Torr.

diffractometer, a LiF monocromator and Cu$K\alpha_1$ radiation. Two types of arrangements are used: low resolution with only a slit between the sample and detector, and high resolution with a Ge(111) analyzer crystal after the sample. The degree of epitaxy in these films was studied using TEM with a point-to-point resolution of 0.18 nm. The film thickness and uniformity were also verified by using profilometry (Alpha-step 200-Tencor Instruments).

3. Results and discussion

The PLD thin films were characterized by FTIR and Raman spectroscopy to investigate the characteristics of infrared and Raman active modes in AlN. AlN with wurtzite structure has nine optical branches [30–32]. At long wavelengths, A_1 and E_1 are the infrared active and A_1, E_1 and E_2 are the Raman active modes. Fig. 2 shows the FTIR absorbance spectrum of the AlN film grown on Si(111) at T_s of 750°C. The data were obtained by computer subtraction of a spectrum of the Si(111) substrate. The strong absorption peak at 665 cm^{-1} is owing to the transverse optical phonon modes of AlN [30–32]. These phonon modes clearly show that the PLD films contain pure AlN phase. The films deposited at all substrate

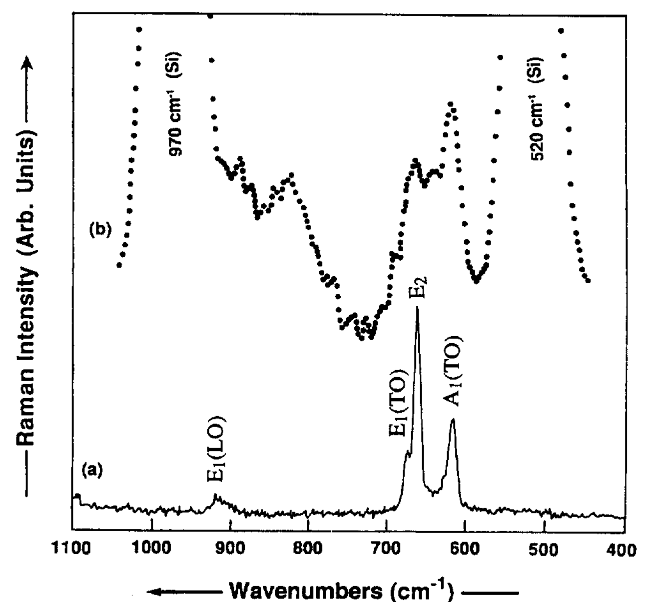

Fig. 3. Raman spectrum of (a) polycrystalline AlN target used for the laser ablation, and (b) 200 nm AlN film deposited on Si(111) at E_D of 3 J cm^{-2}, T_s of 750°C and base pressure of 3×10^{-7} Torr.

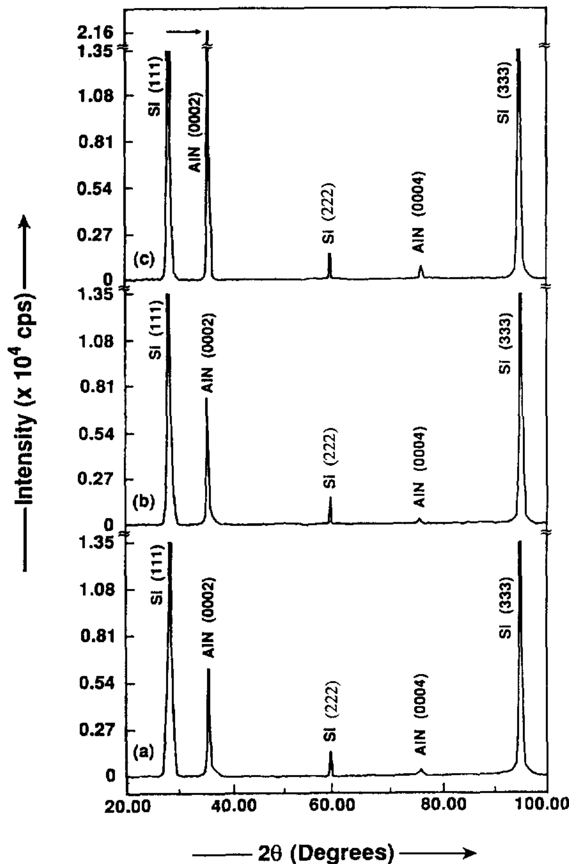

Fig. 4. XRD patterns of the AlN films on Si(111). AlN films were deposited at E_D of 3 J cm^{-2}, base pressure of 3×10^{-7} Torr, and T_s of (a) 550°C, (b) 650°C, and (c) 750°C. The diffraction patterns show peaks from Si(111) family of planes of the substrate and AlN (0002) and AlN (0004) reflections from the AlN film.

temperatures had an IR spectrum characteristic of AlN. Fig. 3(a) shows a typical Raman spectrum of the polycrystalline AlN target used for the laser ablation. In this spectrum, A_1 [TO:610 cm^{-1}], E_2[655 cm^{-1}], and E_1 [TO:667 cm^{-1}, LO:910 cm^{-1}] are the phonon modes of the AlN. These frequencies are in good agreement with the results reported previously [30–32]. Fig. 3(b) shows the Raman spectrum from an AlN film deposited on Si(111) at 750°C. In our study, the phonon propagation vector was along the *c*-axis of the film. In this configuration, the quasitransverse mixed A_1[TO:610 cm^{-1}, LO:893 cm^{-1}], E_1[TO:667 cm^{-1}, LO:910 cm^{-1}, 825 cm^{-1}] and E_2[655 cm^{-1}] modes are expected [30–32]. The Raman spectrum from the AlN film clearly shows the above modes. It should be noted that the relative intensities of A_1, E_1 and E_2 modes are different for the film as compared with the target. This is attributed to the texturing of the AlN film along the *c*-axis normal to the substrate.

Detailed X-ray diffraction measurements (Θ and ω scans) were carried out to study the crystalline properties of the AlN films. Fig. 4 shows "Θ–2Θ" angular scans of the AlN films deposited on Si(111) at three different growth temperatures 550°C (Fig. 4(a)), 650°C (Fig. 4(b)) and 750°C (Fig. 4(c)), E_D of 3 J cm^{-2}, pulse repetition rate of 15 Hz, and base pressure of 3×10^{-7} Torr. The diffraction patterns show expected Si(111) family of planes together with AlN (0002) and AlN (0004) reflections. No other AlN reflection is present indicating that the AlN films deposited at all temperatures are predominantly oriented along the [0001] direction. The lattice constant "*c*" for these films is found to be 0.497 nm which is close to the bulk AlN, i.e. 0.24%. It can also be seen that the integrated intensity of the (0002) peak is low for the film deposited at 550°C and increases as a function of T_s. The substantial increase in the integrated intensity of the (0002) diffraction line corresponding to the AlN film deposited at 750°C indicates that the AlN basal plane, i.e. (0001) plane, is aligned to the (111) plane of the Si substrate. It should be noted that the textured growth along the preferred direction for the films grown at lower temperatures is owing to the minimum surface energy of AlN(0002) relative to the other planes.

The X-ray rocking curve is a powerful technique to determine the epitaxial quality of the films. The distribution of crystals with definite orientation (mosaicity) with respect to the substrate normal is reflected in full-width-at-half-maximum (FWHM) of the rocking curve. The X-ray rocking curves were obtained for the films deposited at 550, 650 and 750°C, and the data are presented in Table 1. For the film deposited at 550°C, the width of the rocking curve was quite broad indicating poor alignment of the *c*-axis with the sub-

Table 1
Summary of process parmeter optimization in PLD and the corresponding properties of AlN films

Substrate for AlN thin film growth	Substrate temperature, T_s (°C)	Nitrogen pressure (Torr)	Laser energy density, E_D (J cm^{-2})	ω-rocking curve FWHM (°)	Band gap E_g of AlN film (eV)
Silicon (111)	650	3×10^{-7}	3	1.9	
	750	3×10^{-7}	3	1.1	
	750	5×10^{-4}	3	1.9	
α-Al_2O_3(0001)	700	5×10^{-7}	3	2.2	
	750	5×10^{-7}	3	1.2	5.8
	800	5×10^{-7}	3	0.21	6.1
	850	5×10^{-7}	3	0.07	6.1
6H-SiC(0001)	750	3×10^{-7}	3	0.25	
	800	3×10^{-7}	3	0.06	

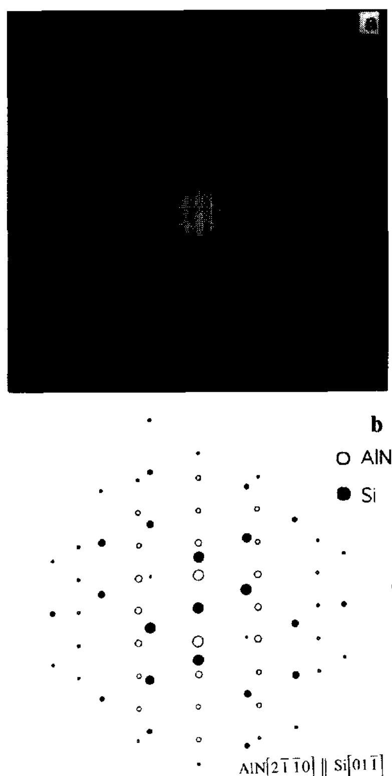

Fig. 5.

strate normal. The alignment of the film with respect to the substrate improved steadily with an increase of T_s. The narrowest rocking curve obtained for AlN films grown on Si(111) substrates at 750°C was ~1.1°.

Fig. 5(a) shows a selected area diffraction pattern from a cross-sectional specimen deposited at 750°C with a base pressure of 3×10^{-7} Torr. The spot diffraction pattern from AlN clearly shows that the film is single crystal. From the simulation (shown in Fig. 5(b)), the epitaxial nature of AlN on Si(111) is established. In the cross-section, AlN[$2\bar{1}\bar{1}0$] is aligned with Si[$01\bar{1}$] axis. In other two directions, we find that AlN[$01\bar{1}0$]||Si[$\bar{4}22$] and AlN[0001]||Si[111]. A similar epitaxial relationship has been reported for AlN films grown on Si(111) by CVD and reactive sputtering [12,15]. The microstructure of the AlN film and the nature of AlN/Si(111) interface were investigated using high-resolution TEM. Fig. 6(a) shows that the AlN/Si(111) interface is quite sharp without any indication of interdiffusion. The alignment of basal plane of AlN with Si[111] is clearly shown in Fig. 6(b). From the lattice fringe spacing, "c" was calculated to be 0.50 nm, very close to the theoretical bulk value of 0.4982 nm, i.e. 0.36%.

The effect of nitrogen partial pressure during laser deposition on the growth quality of AlN films was also investigated. It was found that the total integrated intensity of AlN(0002) X-ray diffraction peak decreases with an increase of nitrogen partial pressure. The intensity of AlN(0002) diffraction peak dropped by a factor of 3 while rocking curve broaden from 1.1 to 1.9° for the film deposited at 750°C and nitrogen partial pressure of 5×10^{-4} Torr as compared with the film deposited at base pressure of 3×10^{-7} Torr and T_s of 750°C (see Table 1). The pressure of the ambient gas significantly affects the reaction kinetics and particulate formation during the time of flight. This is primarily owing to the fact that as the chamber pressure increases, the mean free path in background gas decreases significantly and the number of collisions within the laser induced plasma plume increases. The large number of collisions of the particles in the high background pressure would increase the particulate formation. The particulates grow during the time of flight in the plasma plume and their growth rate increases when the background pressure is increased. In fact, such small particles of <0.1 μm have been observed by Norton et al. [18] in laser ablated AlN films deposited in 50 mTorr pressure of nitrogen and these could be reduced further by lowering the nitrogen partial pressure during deposition. These clusters were deposited randomly on the substrate, causing degradation in epitaxial quality.

The influence of laser fluence and pulse repetition rate on the quality of AlN films was also investigated. Fig. 7 shows the X-ray diffraction pattern obtained from a specimen deposited at 12 J cm^{-2} and T_s of 550°C which contained textured AlN(0001) peaks along with small contribution from AlN(1000) and Al(111). The appearance of Al metal was

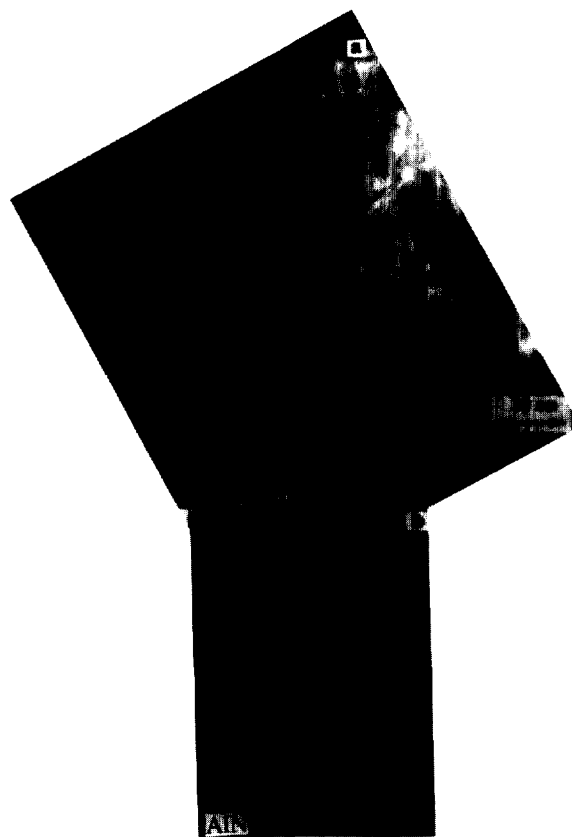

Fig. 6. High resolution TEM: (a) epitaxial AlN film grown on Si(111) at deposition conditions as E_D of 3 J cm^{-2}, T_s of 750°C and base pressure of 3×10^{-7} Torr. (b) Magnified lattice image showing AlN[0001] planes aligned with the Si[111] basal plane. The fringe spacing is ~0.5 nm.

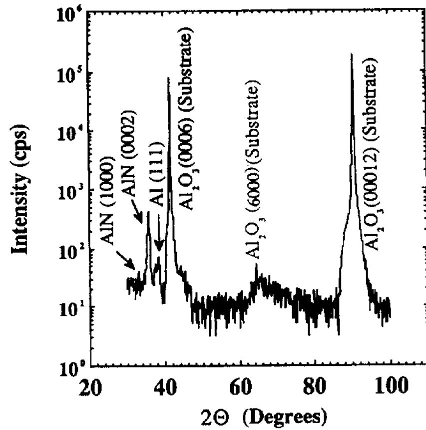

Fig. 7. XRD pattern of the AlN film on sapphire at laser E_D of 12 J cm^{-2} and T_s of 550°C.

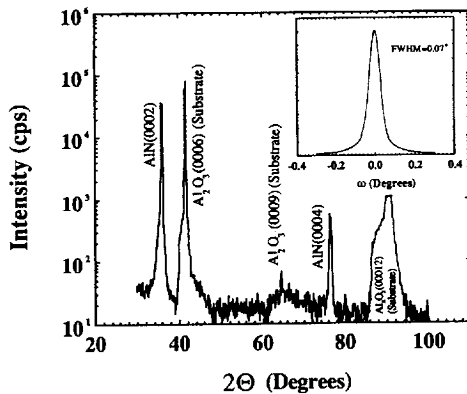

Fig. 8. XRD pattern of the AlN film on Al_2O_3(0001). The film was deposited at a base pressure of 5×10^{-7} Torr, T_s of 850°C, and E_D of 3 J cm^{-2}. The corresponding ω-rocking curve of AlN(0002) peak is shown in the inset.

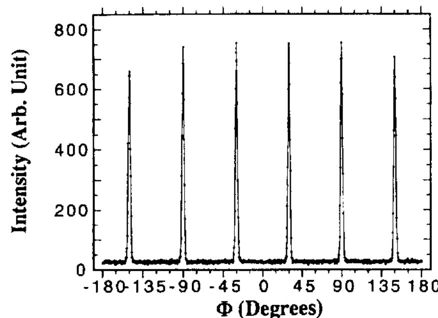

Fig. 9.

owing to the partial decomposition of AlN at higher laser fluence during laser irradiation [33]. At lower laser fluence ≤ 3 J cm^{-2}, however, the single phase AlN was obtained and the decomposition of AlN was minimized. It should be noted that the single phase and fully stoichiometric AlN films can be obtained by ablation of the target in the nitrogen partial pressures, however, it affects the texturing (grain orientation) of AlN and degrades the crystallinity of the c-axis films [11,18]. No significant effect of the pulse repetition rate on the film quality was observed up to 30 Hz, which indicates that films can be grown at higher rates using PLD technique.

Fig. 8 shows XRD "Θ–2Θ" angular scans of the AlN film grown on Al_2O_3(0001) crystal at E_D of 3 J cm^{-2}, T_s of 850°C and base pressure of 5×10^{-7}Torr. The diffraction pattern shows that the AlN film is highly c-axis oriented along [0001] normal of the substrate. The films deposited at T_s as low as 600°C showed similar features except their variation in integrated intensity of AlN(0002) peak lower by two orders of magnitude. The X-ray rocking curves were obtained for the films as a function of T_s and the results are summarised in Table 1. For the film deposited below 700°C, the rocking curve was quite broad indicating a poor alignment of the c-axis with the substrate normal. The alignment of the film with respect to the substrate improved above 700°C. The rocking curve width for AlN film deposited at 850°C on Al_2O_3(0001) was 0.07° (inset of Fig. 8) which indicates excellent alignment of (0001) planes of the AlN with that of substrate. The rocking curve width for Al_2O_3(0006) peak of sapphire substrate was 0.05°. In-plane epitaxy was also determined from Φ scans of {2002} peaks with the phi rotation axis parallel to the c-axis of the films. Fig. 9 shows a plot of Φ scan obtained for the AlN film grown on sapphire(0001) at T_s of 850°C. It shows that the film is epitaxial with a, b axes of the film rotated by 30° from the a and b axes of the sapphire(0001).

TEM was also used to determine the in-plane epitaxial relationship between AlN film and Al_2O_3, and the structure of the interface. Two cross-sectional TEM samples with mutually perpendicular zone axes were prepared. Fig. 10(a)

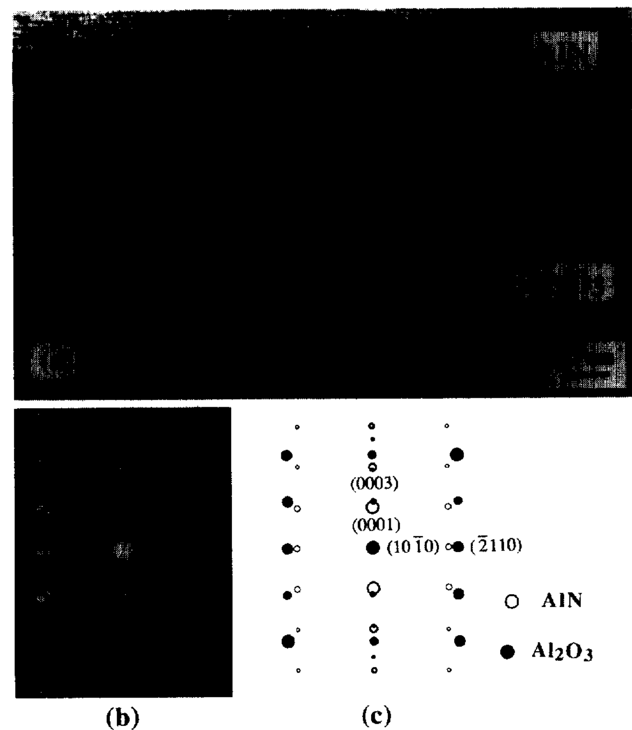

Fig. 10. (a) High resolution TEM image of AlN/Al_2O_3 interface along [01$\bar{1}$0] zone axis: The AlN film was grown at 800°C, laser E_D of 3 J cm^{-2} and without nitrogen partial pressure, (b) corresponding SAD pattern, and (c) simulated diffraction pattern of AlN/Al_2O_3(0001).

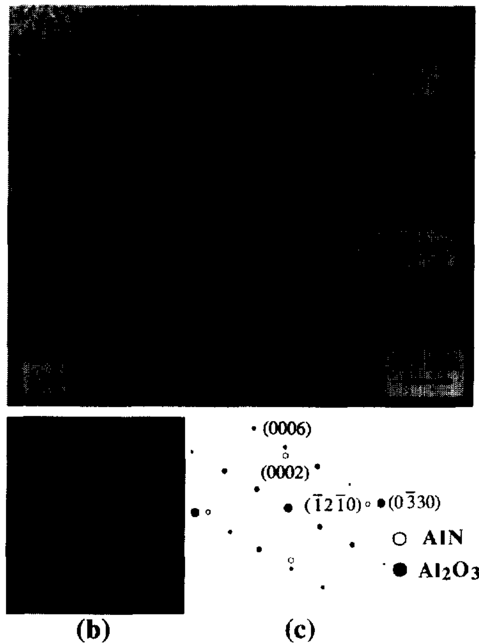

Fig. 11. (a) High resolution TEM lattice image of epitaxial AlN film on $Al_2O_3(0001)$ viewed along $Al_2O_3[1\bar{2}10]$ zone axis, (b) corresponding SAD pattern, and (c) simulated diffraction pattern of $AlN/Al_2O_3(0001)$. The AlN film was grown at E_D of 3 J cm^{-2}, T_s of 750°C and base pressure of 3×10^{-7} Torr.

and (b) show the high resolution lattice image of AlN/Al_2O_3 interface along [$0\bar{1}10$] zone axis and a corresponding selected area electron diffraction (SAD) pattern, respectively. The spot diffraction pattern from AlN clearly shows that the film is single crystal. From the SAD pattern, the epitaxial nature of AlN on $Al_2O_3(0001)$ was established. In the direction of growth, AlN[0001]‖Al_2O_3[0001], while the in-plane epitaxial relationship was found as: AlN[$\bar{1}2\bar{1}0$]‖Al_2O_3[$0\bar{1}10$] and AlN[$10\bar{1}0$]‖ Al_2O_3[$\bar{2}110$]. Similar epitaxial relationships were found by indexing the Al_2O_3[$1\bar{2}10$] zone SAD pattern (Fig. 11(b) and (c)). The in-plane epitaxial relationship (Figs. 10 and 11) shows a 30° rotation of the AlN film with respect to the sapphire substrate in the basal *a–b* plane which is consistent with the results of XRD-Φ scans. These epitaxial relationships are identical with previously reported results of CVD films on sapphire [13]. The high resolution micrographs viewed along Al_2O_3[$0\bar{1}10$] and [$\bar{2}110$] also give a more detailed view of the interface. The $AlN/Al_2O_3(0001)$ interface is clean and quite sharp without indication of interdiffusion. The perfect alignment of basal plane of AlN with $Al_2O_3(0001)$ is clearly observed at the interface. From the lattice fringe spacing, "*c*" was calculated to be 0.497 nm, which is consistent with results of X-ray diffraction. From TEM micrographs, the number density of dislocations was estimated to be $\sim 10^{10}$ cm^{-2}. Such dislocation densities in the material have been shown to be low enough to allow optoelectronic device applications [34].

Fig. 12 shows XRD "Θ–2Θ" angular scans of the AlN film grown on 6H-SiC(0001) crystal at E_D of 3 J cm^{-2}, T_s of 800°C and base pressure of 5×10^{-7} Torr. The diffraction

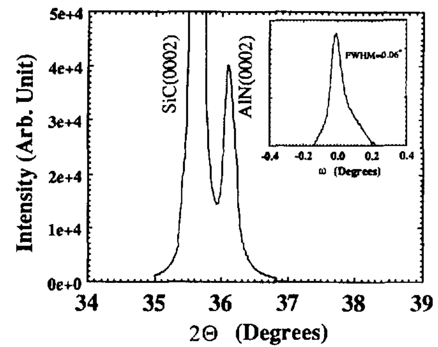

Fig. 12. XRD pattern of the AlN film on 6H-SiC(0001). The ω-rocking curve for the AlN(0002) peak is shown in the inset. The film was deposited at a base pressure of 5×10^{-7} Torr, T_s of 800°C, and E_D of 3 J cm^{-2}.

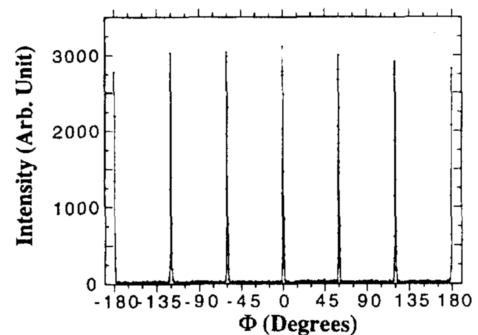

Fig. 13. XRD Φ-scan of {2002} reflections of AlN film grown on SiC(0001) at T_s of 800°C, and E_D of 3 J cm^{-2} and base pressure of 5×10^{-7} Torr.

pattern clearly shows that the AlN film is *c*-axis oriented along [0001] normal of the film plane. The FWHM of the rocking curve for AlN(0002) peak was 0.06° (see inset of Fig. 12). The narrow rocking curve indicates that the film is high quality epitaxial on SiC(0001) substrate. We noted that the lowest temperature for epitaxial growth of AlN on SiC was lower by 100–150°C than that on sapphire and silicon. This could be attributed to smaller lattice mismatch ($\sim 3\%$) between AlN and 6H-SiC. The characteristics of in-plane epitaxy were obtained using Φ scans of AlN film grown on 6H-SiC(0001) and the results are shown in Fig. 13. The peaks at every 60° signify a good alignment of the *a* and *b* axes of the AlN film with that of SiC substrate, i.e. the crystallography was revealed to be AlN⟨1000⟩‖SiC⟨1000⟩.

It is important to note that the lattice parameters of AlN differ quite significantly from that of silicon and sapphire for a lattice matching epitaxy. The lattice misfit ($f_l = 2(b-a)/(a+b)$, where *a* and *b* are the lattice parameters (or interplanar distances) of the substrate and the film, respectively) can be calculated according to epitaxial relationship observed in our experiments. The f_l between AlN and silicon is 22.3%. While in the case of AlN epitaxy on sapphire(0001), the 30° rotation of the film with respect to sapphire in the basal *a–b* plane (as shown in Fig. 14) gives rise to lattice matching of Al–Al (interatomic distance of 0.274 nm) in sapphire to Al–Al (interatomic distance of 0.311 nm) in AlN with misfit of 13.2%. These values of f_l are quite high for lattice matching epitaxy. We have previously demonstrated epitaxial growth

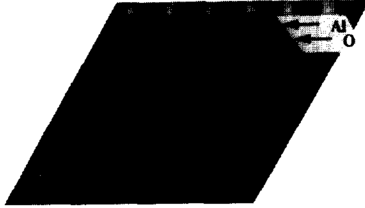

Fig. 14. Simulation of epitaxial relationship between AlN thin film on sapphire substrate showing AlN(0001) crystal structure on sapphire (0001) crystal. The Al–Al atomic distance in the sapphire is 0.274 nm. The bigger hexagon (lattice constant $a = 0.475$ nm) shows the arrangement of the surface atoms (oxygen) in the unit cell of the sapphire (0001) crystal. The smaller hexagon constructed on the sapphire surface will be occupied by Al atoms of the AlN film during epitaxial growth with atomic distance of 0.311 nm. Note that the Al sites in the AlN are identical to that of Al sites in the sapphire and this fact establishes a 30° rotation of the AlN film with respect to the sapphire substrate.

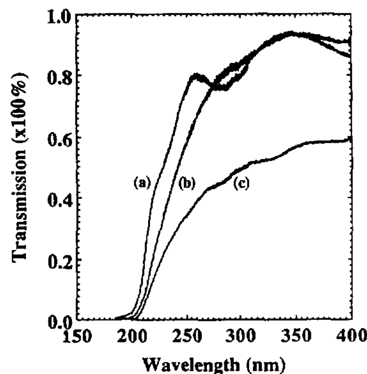

Fig. 15. UV-Visible spectroscopy of *d* are the AlN films on Al_2O_3(0001) deposited at T_s of (a) 800°C and (b) 750°C with laser E_D of 3 J cm^{-2}; and (c) 550°C and E_D of 12 J cm^{-2}.

of large lattice mismatch systems such as TiN on Si and GaAs (100) substrates, and Cu on epitaxial TiN/Si(100) [35–37]. Epitaxial growth in these systems is described in terms of domain matching epitaxy (DME) [10,11,35–38]. The dimensions of the domain become the repeat distance across which lattice matching is maintained. In each domain, "*m*" lattice parameters (or interplanar distances) in the substrate match with "*n*" in the epilayer, where, *m* and *n* are simple integers. This leads to a residual domain mismatch given by "f_d" $= 2(nb - ma)/(nb + ma)$. The lattice mismatch strain "f_l" may be large but the strain associated with the domain given by "f_d" is very small. In case of AlN on Si, four interplanar distances of Si(220) ($4d_{Si(220)} = 0.768$ nm) closely matches with the five interplanar distances of AlN ($5d_{AlN(2\bar{1}\bar{1}0)} = 0.777$ nm) for AlN[$2\bar{1}\bar{1}0$]‖Si[$01\bar{1}$] epitaxial growth, yielding a domain misfit (f_d) of 1.2%. In the case of AlN on sapphire(0001), each domain consisting of 8 Al–Al interatomic distances in AlN matched with each domain of 9 Al–Al interatomic distances in Al_2O_3. This leads to a residual domain misfit (f_d) of 0.7%. Such domain matching epitaxy provides a possible mechanism for epitaxial growth in this system with a large lattice mismatch. This decrease in strain is primarily responsible for domain epitaxial growth.

The optical transmission spectra of the AlN films deposited under various processing conditions are shown in Fig. 15. The curve (Fig. 15(a)) corresponds to the spectrum of epitaxial AlN film deposited at T_s of 800°C and E_D of 3 J cm^{-2}. The film is highly transparent over the wavelength range of interest and it indicates substantial improvement in terms of transmission, absorption edge and its sharpness over the films deposited at T_s of 750°C, and higher $E_D = 12$ J cm^{-2}. The fundamental absorption edge for the epitaxial AlN film was found to be 198 nm which is consistent with the reported value for the high quality films grown on sapphire by MOCVD [14] and SALE [23]. The energy gap, E_g, can be obtained from UV spectrum using Eq. (1).

$$\alpha = [h\omega - E_g]^{1/2}/h\omega \quad (1)$$

where, α is the optical absorption coefficient and the $h\omega$ is the photon energy. The surface light scattering is very large in the UV region as noted by Seki et al. [19]. The α was obtained as described by Seki et al. [19] and Yim et al. [39]. From the dependence of α on photon energy, the E_g was found to be 6.1 eV indicating excellent quality of the film and it is close to that of bulk single crystal AlN(6.2 eV). The lower transmission and broad absorption edge of the film deposited at lower substrate temperatures and higher E_D (curves from Fig. 15(b) and (c)) are attributed to the metallic aluminum content and poor quality of the AlN film as evidenced from XRD results shown in Fig. 7.

The surface morphology of the films was studied by scanning electron microscopy. Fig. 16 shows a typical SEM image of the 250 nm thick AlN film grown on sapphire by PLD at 800°C, laser E_D of 3 J cm^{-2} and base pressure of 5×10^{-7} Torr. It can be seen from this micrograph that the AlN film is extremely smooth with very low density of particulates and without formation of hillocks. The small particulates on the film surface is a common feature of the laser ablation [40]. This surface morphology is comparable with that of films grown by low temperature CVD methods [23,24]. We envisage that the particulates often observed in PLD films can be reduced further by use of a lateral laser beam for inflight vaporization [41]. We also believe that the

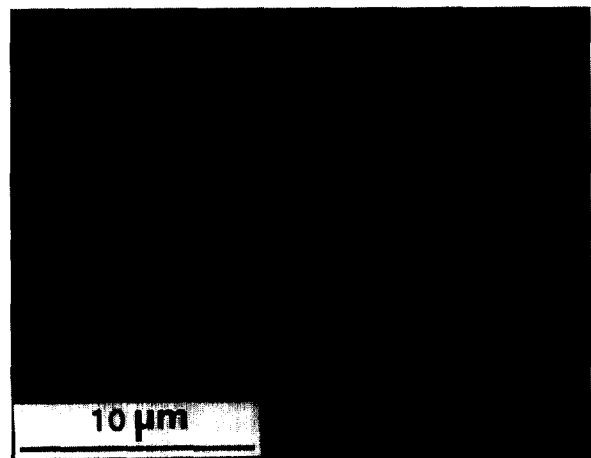

Fig. 16. SEM image of the smooth AlN film (~200 nm thick) grown on Al_2O_3(0001) by PLD. The film was deposited at a base pressure of 5×10^{-7} Torr, T_s of 800°C, and E_D of 3 J cm^{-2}.

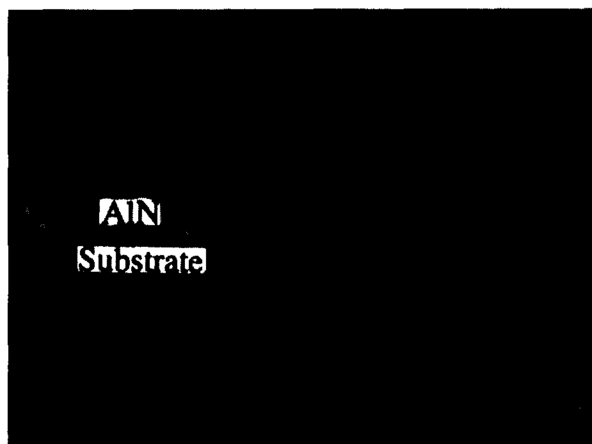

Fig. 17. Cross-sectional SEM image for epitaxial AlN film on sapphire (0001) crystal. The film was deposited at a base pressure of 5×10^{-7} Torr, T_s of 800°C, and E_D of 3 J cm^{-2}.

Fig. 18. SEM image of thick (> 1 μm) and cracked epitaxial AlN film on sapphire (0001) substrate. The triangular crack patterns in the figure attest to the single crystallinity of the AlN layer.

surface morphology and crystallinity of the PLD films under high vacuum conditions were superior to those prepared in high nitrogen partial pressures reported previously [18]. The laser deposition under high nitrogen partial pressures resulted in increase of particle density, and formation of polyhedral spikes on the film surface [18]. The increase of background pressure decreases the plume expansion and decreases the film uniformity as compared with high vacuum depositions. The thickness uniformity of the AlN films was verified by thickness measurements from cross-sectional TEM and SEM samples. The cross-sectional TEM and SEM images showed an optical flat surface of the films. Fig. 17 shows a cross-sectional SEM picture for the AlN film on sapphire. No evidence of columnar structure was observed indicating that the films are epitaxially grown. For thicker AlN films (> 1 μm) cracks were observed along cleavage planes as shown in Fig. 18. The crack propogation geometry indicates that AlN film is essentially a single crystal material.

The film thickness was also verified by profilometry and found to be uniform (about 5%–6% thickness variation) to

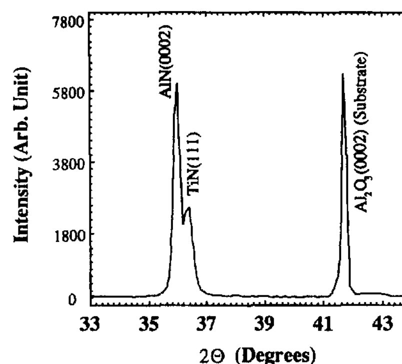

Fig. 19. XRD pattern of the epitaxial AlN(200 nm)/TiN(50 nm)/Sapphire(0001) heterostructure fabricated by pulsed laser deposition.

7–8 mm of the edge of the film. The AlN films prepared by PLD at laser fluence of 2–3 J cm^{-2} and temperature range of room temperature to 850°C were highly insulating with resistivity more than 10^{13} ohm cm^{-1}. However, films deposited at higher laser fluence (i.e. > 10 J cm^{-2}) had resistivities in the range of 7–25 ohm cm^{-1}. The low electrical resistivity of these films deposited at higher laser fluence is owing to Al reach and nitrogen deficient structures and their composite behavior. The electrical resistivity was also measured for Au/AlN/TiN/sapphire (metal–insulator–metal) sandwich structures. Epitaxial AlN/TiN/sapphire(0001) heterostructures were fabricated by in-situ pulsed laser deposition. Fig. 19 shows XRD pattern of heteroepitaxially grown AlN/TiN/sapphire(0001) structure. The epitaxial TiN serves as a contact layer at the bottom as well as a template layer for epitaxial growth of AlN with the *c*-axis normal to the substrate [42] (same as films grown on sapphire). The Au electrodes (50 nm thick) of 1 × 1 mm^2 were deposited on AlN(410 nm)/TiN(50 nm)/Al_2O_3(0001). The electrical resistivity and the breakdown field of these sandwich structures measured from *I–V* characteristics at room temperature were found to be 5–6 × 10^{13} ohm cm^{-1} and 5 × 10^6 V cm^{-1}, respectively.

4. Conclusion

In conclusion, high quality optoelectronic grade epitaxial AlN films were grown on sapphire(0001), 6H-SiC (0001) and Si(111) by PLD technique. The quality of the films was found to depend strongly on the E_D, T_s, and nitrogen partial pressure during deposition. The XRD, UV-visible spectroscopy, electrical resistivity and TEM studies showed that the best films were obtained at $T_s \sim 750$–850°C, $E_D \sim 3$ J cm^{-2} and base pressure ~ 1–5 × 10^{-7} Torr. The FTIR and Raman spectroscopy results clearly established the formation of high quality AlN phase. The FWHM of X-ray rocking curve and the optical absorption edge measured by UV-V spectroscopy for the epitaxial AlN films on sapphire were 0.06° and 198 nm, respectively. The electrical resistivity and the breakdown field of these films were more than 5 × 10^{13} ohm cm^{-1} and 5 × 10^6 V cm^{-1}, respectively. We also established the following film–substrate epitaxial relation-

ship: $AlN[0001] \parallel Al_2O_3[0001]$, $AlN[0001] \parallel Si[111]$, $AlN[0001] \parallel SiC[0001]$ and in-plane alignment of $AlN[\bar{1}2\bar{1}0] \parallel Al_2O_3[0\bar{1}10]$, $AlN[10\bar{1}0] \parallel Al_2O_3[\bar{2}110]$, $AlN[2\bar{1}\bar{1}0] \parallel Si[01\bar{1}]$ and $AlN[0\bar{1}10] \parallel SiC[0\bar{1}10]$. The epitaxial AlN films deposited under optimum growth conditions exhibited a high degree of epitaxy, a sharp interface between the film and the substrate, high resistivity, a sharp absorption edge, and a smooth surface morphology, which is good enough for optoelectronic device applications.

Acknowledgements

The authors gratefully acknowledge K. Jagannadham, S. Oktyabrsky, Hong Wu and Dr. W.D. Fan of our group for helpful discussions. This research was supported by the National Science Foundation (CMS-9414434).

References

[1] H. Morkoc, S. Strite, G.B. Gao, M.E. Lin, B. Sverdlov and M. Burns, *J. Appl. Phys., 76* (1994) 1363.
[2] R.F. Davis, *Proc. IEEE, 79* (1991) 702.
[3] S. Strite and H. Morkoc, *J. Vac. Sci. Technol. B, 10* (1992) 1237.
[4] M.T. Duffy, C.C. Wang, G.D. O'Clock, Jr. S.H. MacFarlance III and P.J. Zanzucchi, *J. Electron. Mater., 2* (1973) 359.
[5] L.M. Sheppard, *Am. Ceram. Soc. Bull., 69* (1990) 1801.
[6] T.J. Mroz, *Am. Ceram. Soc. Bull., 71* (1992) 782.
[7] T.Y. Sheng, Z.Q. Yu and G.J. Collins, *Appl. Phys. Lett., 52* (1988) 576.
[8] G. Selvaduray and L. Sheet, *Mater. Sci. Technol., 9* (1993) 463.
[9] T. Sasaki and T. Matsuoka, *J. Appl. Phys., 77* (1995) 192.
[10] R.D. Vispute, H. Wu and J. Narayan, *Appl. Phys. Lett., 67* (1995) 1549.
[11] R.D. Vispute, J. Narayan, H. Wu and K. Jagannadham, *J. Appl. Phys., 77* (1995) 4724.
[12] Y. Chubachi, K. Sato and K. Kojima, *Thin Solid Films, 122* (1984) 259.
[13] W. Zhang, Y. Someno, M. Sasaki and T. Hirai, *J. Cryst. Growth, 130* (1993) 308.
[14] A. Saxler, P. Kung, C.J. Sun, E. Bigan and M. Razeghi, *Appl. Phys. Lett., 64* (1994) 339.
[15] W.J. Meng, J. Heremans and Y.T. Cheng, *Appl. Phys. Lett., 59* (1991) 2097.
[16] K.S. Stevens, A. Ohtani, M. Kinniburgh and R. Beresford, *Appl. Phys. Lett., 65* (1994) 321.
[17] X. Li and T.L. Tansley, *J. Appl. Phys., 68* (1990) 5369.
[18] M.G. Norton, P.G. Kotula and C.B. Carter, *J. Appl. Phys., 70* (1991) 2871.
[19] K. Seki, X. Xu, H. Okabe, J.M. Frye and J.B. Halpern, *Appl. Phys. Lett., 60* (1992) 2234.
[20] P. Bhattacharya and D.N. Bose, *Jpn. J. Appl. Phys., 30* (1991) L1750.
[21] S.R. Nishitani, S. Yoshimura, H. Kawata and M. Yamaguchi, *J. Mater. Res., 7* (1992) 725.
[22] S. Yoshida, S. Misawa, Y. Fujii, S. Takada, S. Gonda, H. Hayakawa and A. Itoh, *J. Appl. Phys., 53* (1982) 6844.
[23] M.A. Khan, J.N. Kuznia, R.A. Skogman, D.T. Olson, M.M. Millan and W.J. Choyke, *Appl. Phys. Lett., 61* (1992) 2539.
[24] W. Zhang, Y. Someno, M. Sasaki and T. Hirai, *J. Cryst. Growth, 130* (1993) 308.
[25] H. Okano, N. Tanaka, Y. Takahashi, T. Tanaka, K. Shibata and S. Nakano, *Appl. Phys. Lett., 64* (1994) 166.
[26] J. Narayan, N. Biunno, R.K. Singh, O.W. Holland and O. Auchiello, *Appl. Phys. Lett., 51* (1987) 1845.
[27] D.B. Chrisey and G.K. Hubler (eds.), *Pulsed Laser Deposition of Thin Films*, Wiley, New York, 1994; and references cited therein.
[28] K.L. Saenger, *Proc. Adv. Mater., 2* (1993) 1; and references cited therein.
[29] *Pulsed Laser Deposition*, MRS Bulletin, XVII no. 2, 1992.
[30] L.E. McNeil, M. Grimsditch and R.H. French, *J. Am. Ceram. Soc., 76* (1993) 1132.
[31] O. Brafman, G. Lengyel and S.S. Mitra, *Solid State Commun., 6* (1968) 523.
[32] C. Carlone, K.M. Lakin and H.R. Shanks, *J. Appl. Phys., 55* (1984) 4010.
[33] M.J. DeSilva, A.J. Pedraza and D.H. Lowndes, *J. Mater. Res., 9* (1994) 1019.
[34] K. Dovidenko, S. Oktyabrsky, J. Narayan and M. Razeghi, in L. Brus, R.W. Collins, M. Hirose and F. Koch (eds.), *Mater. Res. Soc. Symp. Proc., 395* (1994) 387.
[35] J. Narayan, P. Tiwari, X. Chen, J. Singh, R. Chowdhury and T. Zheleva, *Appl. Phys. Lett., 61* (1992) 1290.
[36] T. Zheleva, K. Jagannadham and J. Narayan, *J. Appl. Phys., 75* (1994) 861.
[37] R.D. Vispute, R. Chowdhury, P. Tiwari and J. Narayan, *Appl. Phys. Lett., 65* (1994) 1.
[38] C.J. Sun, P. Kung, A. Saxler, H. Ohsato, K. Haritos and M. Razeghi, *J. Appl. Phys., 75* (1994) 3964.
[39] W.M. Yim, E.J. Stofko, P.J. Zanzucchi, J.I. Pankove, M. Ettenberg and S.L. Gilbert, *J. Appl. Phys., 44* (1973) 292.
[40] R.K. Singh, D. Bhattacharya and J. Narayan, *Appl. Phys. Lett., 57* (1990) 2022.
[41] G. Koren, R.J. Baseman, A. Gupta, M.I. Lutwyche and R.B. Laibowitz, *Appl. Phys. Lett., 56* (1990) 2144.
[42] R.D. Vispute, J. Narayan, K. Jagannadham and J.D. Budai, *J. Appl. Phys.*, to be submitted.